

# ACETYLCHOLINE RECEPTORS ARE NOT FUNCTIONALLY INDEPENDENT

E. YERAMIAN,\* A. TRAUTMANN,<sup>†</sup> AND P. CLAVERIE<sup>‡</sup>

*\*Unité de Physicochimie des Macromolécules Biologiques, Institut Pasteur, 28, rue du Dr Roux, 75015 Paris, France; †Laboratoire de Neurobiologie, Ecole Normale Supérieure, 46, rue d'Ulm, 75005 Paris, France; and ‡Dynamique des Interactions Moléculaires, Université Pierre et Marie Curie, Tour 22, 4 place Jussieu, 75005 Paris, France*

**ABSTRACT** Analysis of current recordings from acetylcholine-activated channels has largely rested so far on the hypothesis of independence, which states that the opening of one channel does not influence that of its neighbors. We have submitted this assumption to several tests, using as experimental material single channel currents from rat myotubes. We found that, even though the distribution of multiple channel openings may be approximated by the Poisson law, openings are strongly coupled. This conclusion is derived from the analysis of two-time properties associated with patch-clamp data. We show how these properties, which contain more detailed information than the stationary probabilities, can be calculated in practice and why a Poisson analysis is misleading in the present case. The implications of our findings are finally discussed in terms of channel structure and function.

## INTRODUCTION

In the early seventies, the independence in the opening of acetylcholine-activated channels was merely a necessary hypothesis for the interpretation of noise data (Katz and Miledi, 1972; Anderson and Stevens, 1973). This hypothesis was then tested on single channel currents by Neher et al. (1978). These authors found that the stationary probabilities that 1, 2, ...  $n$  channels are open at the same time follow a Poisson distribution. The goodness of the fit was considered sufficient to conclude that the hypothesis of independence used in noise analysis was correct, and that there were no interactions between neighboring receptors.

We have reinvestigated this point for two reasons. First, as will be shown in this paper, stationary probabilities can only be used in tests of very low discriminatory power. Second, we were intrigued by the frequency of events such as those shown in Fig. 2, showing apparently simultaneous openings or closings of two channels. We will show that, although the stationary probabilities of multiple channel openings follow a Poisson distribution, there is a clear interaction between receptors, and that there is some increased probability that another opening will occur during the time a first channel stays open. This result will be demonstrated by using two-time properties (two-time probabilities and transition probabilities).

## METHODS

Rat myotubes were cultured as described previously (Siegelbaum et al., 1984). The experiments were performed at room temperature. The composition of the bath was (in millimolars): 115 NaCl, 2.5 KCl, 2 CaCl<sub>2</sub>, 2 MgCl<sub>2</sub>, 11 glucose, 5 HEPES at pH 7.4. Single-channel

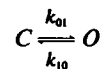
recordings were performed in the cell-attached configuration (Hamill et al., 1981). The pipette solution was identical to the bath solution, but without glucose, and plus 200 or 300 nM acetylcholine (ACh). Channel currents were recorded with a FM tape recorder and later digitized at 5–10 kHz (after a 8-pole Bessel filtering at one fourth of the sampling frequency) and analyzed on an LSI 11/23 computer.

The closed times distributions show two clearly distinct components pertaining to different mechanisms. The slow component (time constant: several tens of milliseconds) corresponds to the interval between two different channel openings. The fast component (briefer than one millisecond) is probably due to fast oscillations of the same channel between the open and closed conformations (Colquhoun and Sakmann, 1981). In the definition of the channel open time we ignore closed periods briefer than 2 ms, i.e., 3–5 times the time constant of the fast component of the closed times distribution. The analysis of the two-time properties has been done both before and after cancelling these fast oscillations. As will be discussed later, both procedures give similar results.

## THEORY

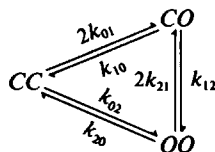
### Two Schemes of Channel Activation

In this paper, several experimental probabilities will be compared with the values predicted in two schemes. Scheme I is the simplest independence model, which states that each channel can adopt, independently of the others, two states, closed ( $C$ ) or open ( $O$ ).



Scheme I

Scheme II is a dimeric model, which is one simple manner of taking into account channels presenting a nonindependent activation.



Scheme II

CC, CO, and OO represent the conformations of one dimer of channels with either 0, 1, or 2 channels open. There are two conformations corresponding to CO, so the effective transition rates characterizing the passage to this state are noted  $2k_{01}$  and  $2k_{21}$ .

These schemes are certainly oversimplified since the nicotinic receptor may adopt several closed and several open states. For example, one common scheme of activation of the ACh receptor is of the form

$$C_0 = C_1 = C_2 = O,$$

where the various  $C_i$  represent closed states of the receptor with  $i$  ACh molecules bound. Such a scheme can be brought back to a two-state model by considering the different closed states as a whole. The apparent macroscopic rate of opening,  $K_{app}$  will be related to the true microscopic rate of opening  $\beta$  by

$$k_{app} = n \cdot \frac{P_{C_2}(\infty)}{\sum_i P_{C_i}(\infty)} \cdot \beta,$$

where  $n$  is the number of functional channels and  $P_{C_i}(\infty)$  the stationary probability of a channel to be in the  $C_i$  state (see below).

A similar reasoning can be used to treat the case of a homogeneous population of channels with several open states (see e.g. Colquhoun and Sakmann, 1981; Takeda and Trautmann, 1984; Sine and Steinbach, 1984).

A further complication may arise from the existence of heterogeneous populations of subunits (as regard to kinetic behaviors). This specific problem will be dealt with in the course of the paper (see Appendices I and II).

In summary, the question of the independence of the receptors can be fruitfully examined by comparing the predictions of Schemes I and II to the experimental data.

### Stationary Probabilities

If each channel in a large population has the same low probability of being activated, the stationary probability  $P_j(\infty)$  that  $j$  independent channels are open together is given by the Poisson law

$$P_j(\infty) = e^{-\mu} \cdot \frac{\mu^j}{j!},$$

where  $\mu$  is the mean number of open channels.

If the channels are not independent but function as dimers (Scheme II), each element in a population of  $n$  dimers is characterized by three states: two closed channels (probability  $1-P-Q$ ), one open channel (probability  $P$ ) or two open channels (probability  $Q$ ). A total number of  $j$  open channels can result from several combinations of  $j_1$  dimers with one open channel, and  $j_2$  dimers with two open channels. Let  $\mu_1$  be the mean number of dimers with one channel open ( $\mu_1 = nP$ ) and  $\mu_2$  the mean number of dimers with two channels open ( $\mu_2 = nQ$ ). A stationary probability in a bi-Poisson law is given by

$$P_j(\infty) = \sum_{\substack{j_1, j_2 \\ j_1 + 2j_2 = j}} (e^{-\mu_1} \cdot \mu_1^{j_1} / j_1!) (e^{-\mu_2} \cdot \mu_2^{j_2} / j_2!).$$

One condition of application of both laws is that the number of channels in a patch is large. Is this a reasonable assumption in our experimental conditions?

### Number of Channels in a Patch

The number of toxin binding sites in the membrane of myotubes is of the order of  $10^2$ – $10^3/\mu\text{m}^2$  (Land et al., 1977). The area of patch of membrane, invaginated in a pipette with a tip of 2–3  $\mu\text{m}$  in diameter, is of the order of 5–20  $\mu\text{m}^2$  (Sakmann and Neher, 1983). The number of receptors per patch is thus of the order of  $10^3$ – $10^4$ . In the continuous presence of ACh, a fraction of these receptors is desensitized (Katz and Thesleff, 1957; Feltz and Trautmann, 1982), and thus not functional. An estimate of the number of functional channels,  $n$ , in the presence of 200 nM ACh can be obtained from the average frequency of channel opening ( $f$ ), the mean open time of the channel ( $\tau$ ), and the estimated fraction of open channels ( $y$ ), such that  $n = f \cdot \tau / y$ . In the experiments illustrated here, the range of values were 10–40  $\text{s}^{-1}$  for  $f$  and 8–20 ms for  $\tau$ . For an exact determination of  $y$ , one should know the value of the microscopic dissociation constant of ACh from each binding site, and of the isomerisation constant of a receptor that has bound two ACh molecules. These values are unknown, but the ACh concentration where a channel is open half of the time has been evaluated as 6  $\mu\text{M}$  (Siegelbaum et al., 1984). This allows to estimate that, in the presence of 200 nM ACh, the fraction of open channels,  $y$  should be  $1$ – $2 \times 10^{-3}$  of all the functional channels.

From these values, one can estimate that in the continuous presence of 200 nM ACh, 40–800 channels are functional in a patch. Given the experimental uncertainties and the existence of desensitization, this estimate is in reasonable agreement with the values of toxin binding sites given above.

### Two-time Probabilities

The main conclusions of this paper will be based on the analysis of two-time properties. Two-time probabilities are

defined as  $P_{ij}(\tau) = \text{Prob}(\text{State } j \text{ at time } t + \tau \text{ and state } i \text{ at time } t)$ .

A state  $i$  is characterized by the fact that  $i$  channels are simultaneously open. The process  $X(t)$  considered is supposed to be a homogeneous Markov process, which means that  $P_{ij}(\tau)$  is independent of the initial time  $t$ . Obtaining the two-time probabilities  $P_{ij}(\tau)$  was done by the computerized realisation of the process illustrated in Fig. 1. A "ruler" of length  $\tau$  was shifted by steps equal to the sampling interval  $\Delta T$  along a time-axis. Let  $N_{ij}$  be the number of steps where the ruler has its origin on an  $i$  level and its end on a  $j$  level,  $T = N \cdot \Delta T$  the total duration of the recording and  $\tau = k \cdot \Delta T$ , one has  $P_{ij}(\tau) = N_{ij} / (N - k)$ . This procedure amounts to evaluate the two-time probability  $P_{ij}(\tau)$  as the time average of the function  $X_{ij}(t)$

$$X_{ij}(t) = \begin{cases} 1 & \text{if } X(t) = i \text{ and } X(t + \tau) = j \\ 0 & \text{otherwise} \end{cases}$$

and

$$P_{ij}(\tau) = \langle X_{ij}(t) \rangle = \lim_{T \rightarrow \infty} \frac{1}{T} \int_0^T X_{ij}(t) dt.$$

For a recording of length  $T$  the above limit is supposed to be reached when a satisfactory convergence is obtained. With the limitation  $t + \tau = T$ , one may write

$$\begin{aligned} P_{ij}(\tau) &= \frac{1}{T - \tau} \int_0^{T-\tau} X_{ij}(t) dt \\ &= \frac{1}{T - \tau} \sum_{l=0}^{N-1-k} \int_{l\Delta T}^{(l+1)\Delta T} X_{ij}(t) dt \\ &= \frac{1}{(N - k)\Delta T} \sum_{l=0}^{N-1-k} \Delta T \cdot X_{ij}(l, l + 1) \\ &= \frac{1}{N - k} \sum_{l=0}^{N-1-k} X_{ij}(l, l + 1). \end{aligned}$$

$X_{ij}(l, l + 1)$  denotes the value taken by  $X_{ij}(t)$  (0 or 1) for  $t$  belonging to the interval  $(l\Delta T, (l + 1)\Delta T)$  and

$$\sum_{l=0}^{N-1-k} X_{ij}(l, l + 1) = N_{ij}$$

is the number of steps  $\Delta T$  crossed by the ruler with its origin on a  $i$  level and its end on a  $j$  level. An example of this process is given in Fig. 1 (the corresponding computer program, in Fortran, may be provided on request).

The theoretical functions  $P_{02}(\tau)$  were calculated after their spectral expansion. Thus, in both schemes of channel activation,  $P_{02}(\tau)$  may be written in the form

$$P_{02}(\tau) = A_0 + A_1 \cdot e^{-\lambda_1 \tau} + A_2 \cdot e^{-\lambda_2 \tau}.$$

If large numbers of channels (or dimers of channels) are

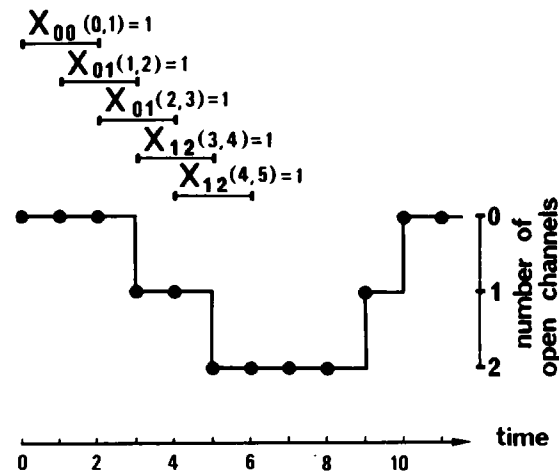


FIGURE 1 Practical obtention of a two-time probability. The points give an idealized representation of the digitized data (kept in a table) used to estimate the two-time properties of the single channel currents. The time unit is the sampling interval,  $\Delta T$ . A "ruler" of length  $\tau = 2 \Delta T$  can be shifted 10 times (5 of which are shown), with a  $\delta T$  step. There are two steps  $[l\delta T, (l+1)\delta T]$ , for which the ruler has its origin on the level 0 and its end on the level 1  $[(1, 2) \text{ and } (2, 3)]$ , so that  $P_{01}(2\delta T) = 2/10 = 1/5$ . See text for the definition of the function  $X_{ij}(l, l + 1)$ .

considered, one should add to this expression other exponential terms with smaller and smaller amplitudes.

### Transition Probabilities

Transition probabilities are defined by  $P_{ij}(\tau) = \text{Prob}(\text{state } j \text{ at time } t + \tau / \text{state } i \text{ at time } t)$ .

Each  $P_{ij}$  is a conditional probability that is closely related to the two-time probability  $P_{ij}(\tau)$  through the relationship

$$P_{ij}(\tau) = P_{ij}(\tau) / P_i(\infty),$$

in which  $P_i(\infty)$  is the stationary probability of state  $i$ . Transition rate  $K_{ij}$  can be derived from the transition probabilities by

$$K_{ij} = \lim_{\tau \rightarrow 0} P_{ij}(\tau) / \tau \quad \text{when } \tau \rightarrow 0.$$

The observed effective transition rates, which are model-independent values, are related to the microscopic rate constant  $k_{ij}$  by relations that depend upon the number of functional receptors in the patch and on the model chosen to describe the activation of these receptors. In the independence model, the transition rates are given by

$$K_{01} = nk_{01} \quad \text{and} \quad K_{12} = (n - 1)k_{01}.$$

In this equation,  $K_{12}/K_{01}$  is necessarily smaller than 1. In Scheme II, the transition rates are given by

$$K_{01} = n \cdot 2k_{01} \quad \text{and} \quad K_{12} = (n - 1) \cdot 2k_{01} + k_{12}$$

so that

$$\frac{K_{12}}{K_{01}} = 1 + \frac{1}{n} \cdot \left( \frac{k_{12}}{2k_{01}} - 1 \right).$$

In this theoretical scheme,  $K_{12}/K_{01}$  can be larger than 1.

In this treatment we have examined the case of a single population of homogeneous channels. The possible effect of a heterogeneity in the channel population on the ratio  $K_{12}/K_{01}$  is examined in Appendix I. The conclusion of this appendix is that an experimental ratio  $K_{12}/K_{01} > 1$  indicates the presence of at least one population of nonindependent channels.

## RESULTS

Fig. 2 illustrates typical events observed in a patch, in the presence of 200 nM ACh. As expected from a homogeneous channel population, openings have a constant amplitude and open time durations are exponentially distributed, apart from a slight excess of brief events. But the independence of these channels may be questioned, in view of the frequent occurrence of pairs of channels that seem to open

or close simultaneously, like those shown in Fig. 2 *a*. To determine whether this apparent simultaneity results from mere coincidence or not, we have measured several probabilistic parameters in our recordings and compared them to the predictions of the two schemes given in the Theory section.

## Stationary Probabilities

As shown above, the number of functional channels per patch and the probability of opening of each channel are such that the conditions of application of a Poisson test are fulfilled. Table I gives the stationary probabilities  $P_j(\infty)$  that  $j$  channels are open in one patch. The experimental values are compared to the Poisson and bi-Poisson predictions.

As already described (Neher et al., 1978), we can see in Table I that a Poisson distribution satisfactorily fits the experimental values of the stationary probabilities. If instead of being independent the channels behave as functional dimers (Scheme II), the same stationary probabilities should follow a bi-Poisson law rather than a Poisson

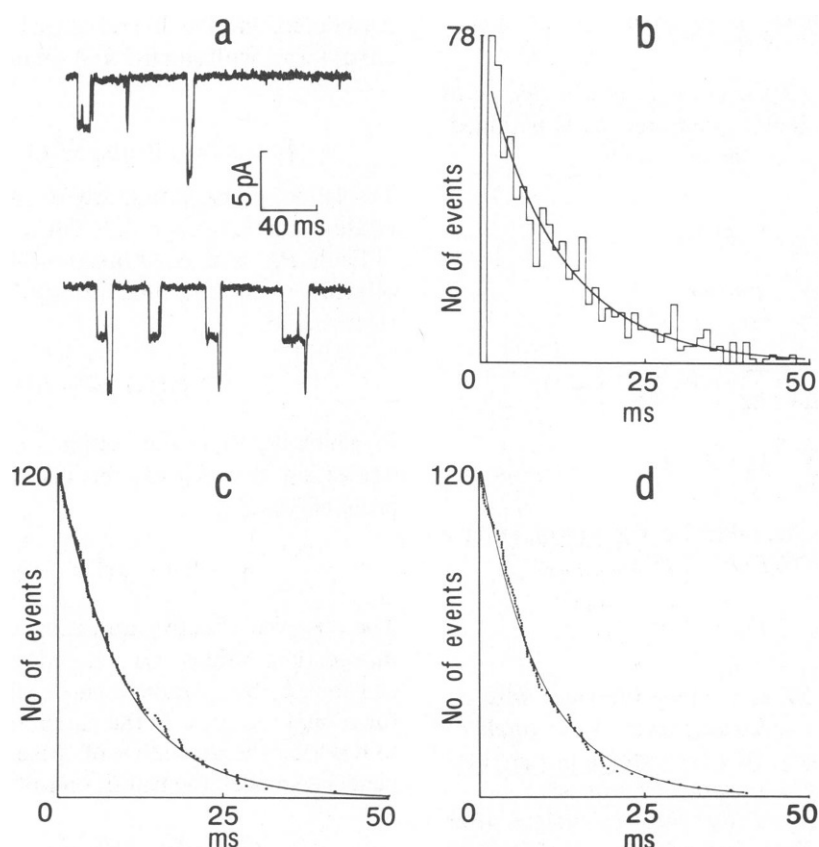


FIGURE 2 Analysis of one recording of ACh-activated channels (sampling frequency 5 kHz; filter 1.5 kHz except in *a*). (*a*) Channels recorded in a rat myotube, in the presence of 200 nM ACh. The potential of the patch, calculated as the difference between the estimated resting potential of the cell and the pipette potential was -110 mV. The data were filtered at 3 kHz. (*b*) Distribution of the durations of the same channel openings (after discarding the transient closures more brief than 2 ms). The exponential fit has a time constant of 10.8 ms. (*c*, *d*) Cumulative histograms of first latencies  $I_1$  (*c*) and  $I_2$  (*d*) (see text for definition), i.e., number of latencies more brief than the duration given in abscissa. The time constants of the exponential fits are 9.7 (*c*) and 8.9 ms (*d*).

TABLE I  
POISSON AND BI-POISSON ANALYSIS OF THE  
STATIONARY PROBABILITIES  $P_j(\infty)$  THAT  $j$  CHANNELS  
( $j = 0$  TO 4) ARE OPEN IN ONE PATCH IN THE  
PRESENCE OF 200 nM ACh

Experimental values	0.7208	0.231	0.043	0.0033	0.0018
Poisson predictions	0.7159	0.2392	0.0399	0.0044	0.00037
Bi-Poisson predictions	(1.007)	(0.966)	(1.077)	(0.75)	(4.86)
	0.7208	0.231	0.042	0.0055	0.00057
	(1)	(1)	(1.024)	(0.6)	(3.16)

The experimental values are the proportion of total recording time when  $j$  channels are open. The mean value  $\mu$  used in the Poisson law ( $P_j(\infty) = e^{-\mu} \cdot \mu^j / j!$ ) was estimated as the mean number of channels open at one time, averaged over the whole record. The ratios  $P_j(\infty)$  experimental/ $P_j(\infty)$  predicted are given between brackets. For the bi-Poisson analysis,  $\mu_1$  and  $\mu_2$  were estimated from the experimental values of  $P_0(\infty)$  and  $P_1(\infty)$ .

law. It appears in Table I that the experimental values can be fitted equally well by both laws. This result, shown in one case, was also obtained in six other cases tested. One could wonder how Scheme II can lead to stationary probabilities apparently not different from those predicted in Scheme I. One first answer is that a difference with an independent behavior could exist, but because of the large number of channels, concerted transitions (of neighbor channels) are diluted among independent transitions (of distant channels), so that the difference with an independent behavior falls below the limit of detection of experimental measurements. The second possible answer is that theoretically a set of six rate constants in Scheme II, with the condition that the openings are not independent ( $k_{12} \neq k_{01}$ ), can give stationary probabilities that exactly follow a Poisson distribution. This can be shown in the simple case of two channels, and the following result may be easily generalized to a population of  $N$  such subunits.

In the case considered there are three stationary probabilities  $P_0(\infty)$ ,  $P_1(\infty)$ , and  $P_2(\infty)$ . Let  $p$  be the elementary probability for a channel to be open ( $p = k_{01}/k_{01} + k_{10}$  in Scheme I). If the two channels are independent, then the binomial law (which can be approximated by the Poisson law when  $N$  is large) may be used and it gives

$$\begin{aligned} P_0(\infty) &= (1 - p)^2 \\ P_1(\infty) &= 2p(1 - p) \\ P_2(\infty) &= p^2. \end{aligned} \quad (1)$$

The converse reasoning would state that independence holds as soon as one finds some  $p$  that gives back the  $P_j(\infty)$  according to Eq. 1. Such a reasoning has been used, for example by Tank et al. (1982), to assess the independence of two Cl protochannels coupled in a dimer unit. This converse reasoning is false.

The same stationary probabilities can indeed be derived from Scheme II with an infinite set of parameters  $k_{ij}$ . In Scheme II the stationary probabilities have the following

expressions

$$\begin{aligned} P_0(\infty) &= \frac{N_0}{D} \\ P_1(\infty) &= \frac{N_1}{D} \\ P_2(\infty) &= \frac{N_2}{D} \end{aligned} \quad (2)$$

with

$$\begin{aligned} N_0 &= 2k_{10}k_{21} + k_{20}k_{10} + k_{20}k_{12} \\ N_1 &= 2k_{20}k_{10} + 4k_{21}k_{01} + 2k_{21}k_{02} \\ N_2 &= 2k_{01}k_{12} + k_{02}k_{10} + k_{02}k_{12} \\ D &= N_0 + N_1 + N_2. \end{aligned}$$

For any given  $p$  it is very easy to set the desired relation between the opening rate constants (for example  $k_{12} = 25k_{01}$ ) in Scheme II and two more arbitrary conditions (for example  $k_{02} = k_{20} = 0$ ) and still solve the system of equations that allows to account for relations (1) with stationary probabilities of Scheme II (for the example above, one solution is  $k_{12} = \frac{5}{2}p$ ,  $k_{01} = p/10$ ,  $k_{21} = \frac{5}{2}(1 - p)$ , and  $k_{10} = 1 - p/10$ ).

### First Latencies Histograms

Next, it was reasoned that more information could be gained if, instead of considering the averages of several states (0, 1, 2... channels open), one examined how the transitions from one state to another take place. To this end we first analyzed the distributions of two latencies  $l_1$  and  $l_2$ , in seven different records.  $l_1$  is the first latency of opening to level 2 (2 channels open) after an initial opening to level 1.  $l_2$  is the latency of closing to level 0 after a closing to the level 1.

The distributions of  $l_1$  and  $l_2$  for one cell are shown in Fig. 2 c, d. Both values are exponentially distributed, with time 9.7 constants and 8.9 ms, respectively. This difference is not significative: the ratio of the two time constants (1.09 in this case) was  $1.02 \pm 0.12$  (mean  $\pm$  SD) for the seven recordings where it was measured. These results are compatible with both schemes. In Scheme I, both durations should equal the inverse of the rate at which level 1 is left; this rate is the sum of all the rates that lead away from this state, toward either level 0 or level 2

$$1/l_1 = 1/l_2 = K_{10} + K_{12}.$$

The situation will be identical for Scheme II, if the direct transitions  $0 \rightarrow 2$  and  $2 \rightarrow 0$  do not occur at a measurable rate. If they did, the amplitude of the first bin of the histogram (or the ordinate of the first point of the cumulative histogram) should lie above the exponential. These histograms then imply that no more than 5–10% of the transitions to/from level 2 occur directly with level 0.

Direct transitions occurring at a lower frequency cannot be detected with this approach (a much larger number of transitions should be measured to improve this detection threshold).

However, these latencies histogram do not tell us if, in the case of Scheme II,  $k_{01}$  and  $k_{12}$  are identical or not, and the question of the independence in the activation process cannot be answered by this approach.

## Two-time Probabilities

We then analyzed two particular two-time probabilities  $P_{02}(\tau)$  and  $P_{20}(\tau)$ , which have been defined in the Methods section. The two-time probabilities  $P_{02}(\tau)$  and  $P_{20}(\tau)$  obtained in seven different experiments are illustrated in Fig. 3 (*a* and *b*). The data (circles) are fitted with a polynomial regression of the third degree (dotted line), which will be discussed below. Between 0.2 and 1.2 ms the data can also be fitted empirically with a straight line. If the channels were independent, both curves should display parabolic behaviors with zero slopes at the origin. This is because in this case,  $P_{02}(\tau)$  would be related to  $P_{01}(\tau)$  through a relation of the form:  $P_{02}(\tau) = A(P_{01}(\tau))^2$  (at least for small  $\tau$  values).

As  $P_{01}(\tau)$  is proportional to time (for  $\tau \rightarrow 20$ ),  $P_{02}(\tau)$  should be proportional to the square of time (see Appendix II). This result is a first suggestion that Scheme I (independent channels) is incorrect. Interestingly, in this Appendix it is also shown that this criterion hoods for the addition of several populations of independent channels.

Fig. 3 *c* shows the probabilities  $P_{02}(\tau)$  obtained by simulation of Schemes I and II, on a number of events similar to that used in the experimental cases. To realize the transition rates for each individual subunit, a random generator was used. To avoid some spurious correlations observed with usually available generators, a generator endowed with the property of high degree equidistribution (Postnikov, 1973) was implemented on the computer (a study of these specific problems is to be reported elsewhere). The simulation of Scheme I (independent channels), shown by the triangles, gives a parabola, whereas the simulation of Scheme II (dimers of channels), shown by the circles, gives a curve very similar to that in Fig. 3 *a*. Fig. 3 *d* illustrates the probabilities  $P_{02}(\tau)$  obtained by analytical calculations based on Schemes I and II. The symbols give the exact values of  $P_{02}(\tau)$  as sums of exponentials, calculated after their spectral expansion (Cox and Miller, 1965; Colquhoun and Hawkes, 1977). The continuous line underlines the apparent linearity of part of the curve obtained from Scheme II; linearity is of course not expected a priori from a sum of exponentials. This feature becomes clearer when one uses the power series expansion of  $P_{02}(\tau)$  rather than its exact value. For small values, an expansion truncated at the third order is sufficient, which gives

$$P_{02}(\tau) = a + b\tau + c\tau^2 + d\tau^3.$$

Accordingly, in Fig. 3 *d*, the dotted lines represent a third order polynomial fitting of the exact values of  $P_{02}(\tau)$ .

For independent channels, the parabolic aspect of the curve reflects the fact that in this case,  $c \gg b$ , ( $c/b = 30.3$  for the curve corresponding to Scheme I). On the contrary, for dimers of channels, this condition does not hold anymore, due to the presence of a genuine coefficient  $b$ , which is not negligible compared to  $c$ , hence the linearity of part of this curve ( $c/b = 0.04$  for the curve corresponding to Scheme II). In the polynomial regression of the experimental data (Fig. 3 *a*) the value of the ratio  $c/b$  was 0.24, which is clearly not consistent with Scheme I, but is compatible with Scheme II. It must be mentioned that in all cases, the slope of the empirically drawn straight line is larger than the coefficient  $b$ . In other words, the linear approximation, which does not go through the axis origin, does not give the slope of the curve when  $\tau \rightarrow 20$ : to recover a satisfactory estimate of this slope of the curve at the origin, it is necessary to resort to a polynomial approximation of sufficient order.

A series of analytical calculations were done with various sets of parameters. They reveal that a linear component in the curves  $P_{02}(\tau)$  and  $P_{20}(\tau)$  can only be obtained by setting  $k_{02}$  and  $k_{20}$  different from zero. Even rate constants ten times smaller than those used in Fig. 3 *d* can yield this linear component. On the contrary when  $k_{02}$  is zero, a linear component cannot be obtained whatever the value of the ratio  $k_{12}/k_{01}$ .

In summary, the curves representing the two-time probabilities  $P_{02}(\tau)$  and  $P_{20}(\tau)$  exhibit a linear part that is particularly evident by inspecting the coefficients of their polynomial regression. This linear part is incompatible with Scheme I. In Scheme II it implies necessarily that  $k_{02}$  and  $k_{20}$  are different from zero.

Interestingly, with the values adopted in Fig. 3 *d*, if  $k_{12}$  is set equal to  $k_{01}$  and  $k_{21}$  equal to  $k_{10}$ , the effective linear part goes through the origin, leading to a single straight line throughout the interval [0–2] ms. This feature would be indicative of the fact that in the experimental case there should also be a departure from the independence scheme through the conditions  $k_{12} \neq k_{01}$  and/or  $k_{21} \neq k_{10}$ . This point will be investigated in more detail in what follows.

## Transition Probabilities and Transition Rates

The two-time probabilities can give an information on a process lasting for any duration (here several milliseconds), but their quantitative analysis is not easy. Thus, we examined another parameter, the transition rate from one state to another, which is not independent from the previous one but differs from it on two points: it restricts the analysis to the shortest measurable time after one transition, but it allows an accurate quantitative analysis. The rate of transition from one state to another can be derived from the transition probabilities  $P_{ij}(\tau)$ , which have been defined in the Theory section. These transition rates

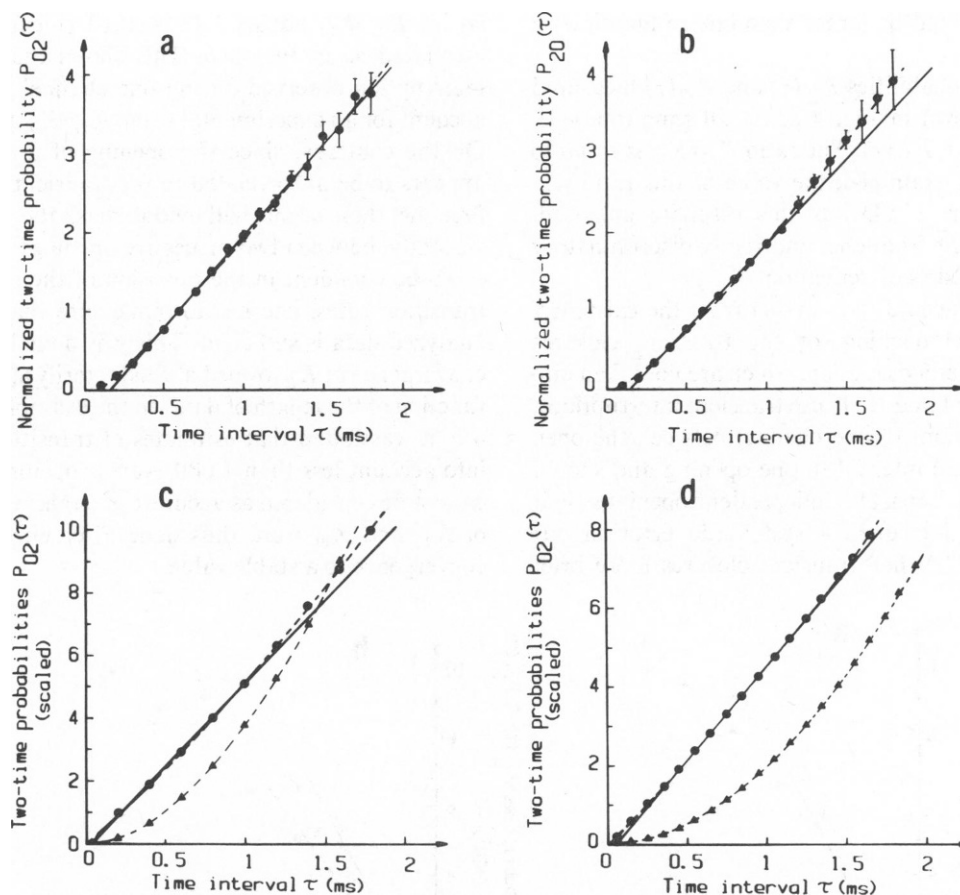


FIGURE 3 Two-time probabilities from experimental data (*a, b*), simulations (*c*) and calculations (*d*). (*a, b*) Probabilities averaged from the data of seven cells ( $\bullet$ ), as described in the text. The recordings were made in the cell-attached mode at an estimated patch potential of  $-90 \pm 20$  mV. The data were sampled at 5 kHz (three experiments) or 10 kHz (four experiments) and filtered at one fourth of the sampling frequency. The filtering introduces time lags of 0.2 and 0.1 ms, respectively, which were corrected for. To average the results of different experiments, in *a* and *b*,  $P_{02}$  and  $P_{20}$  were arbitrarily set to 1 for  $\tau = 0.6$  ms. The bars give the standard deviation when its value exceeds the size of the symbol. In *a, b, c*, and *d*, the dotted curves give the third degree polynomial regression of the data; straight lines were fitted by eye. (*c*) Simulated probabilities  $P_{02}(\tau)$  for a population of independent channels (triangles) and for functional dimers (circles). The two simulations were done for the equivalent of a duration of 100 s, with the rate constants given below. The ordinates are multiplied by  $10^4$  (circles) and by  $5 \cdot 10^4$  (triangles). (*d*)  $P_{02}(\tau)$  was calculated for a dimer (circles) and for two independent channels (triangles), with the rate constants given below. The ordinates were multiplied by  $10^5$  (triangles) and  $10^4$  (circles).

Values of the rate constants ( $s^{-1}$ ) used in simulations and calculations

	Fig. 3c	Fig. 3d
$k_{01}$	0.5	5
$k_{10}$	50	50

#### Scheme I

$k_{01}$	0.5	5
$k_{10}$	50	50
$k_{12}$	5	20
$k_{21}$	100	67
$k_{02}$	0.05	0.5
$k_{20}$	6	5

#### Scheme II

can be used to discriminate between Schemes I and II. More precisely, the experimental value of the ratio  $K_{12}/K_{01}$  will be compared to unity; as shown in the Theory section, this ratio should be less than one in the independence model, but could be larger than one in the dimeric one.

The transition probabilities  $P_{01}(\tau)$  and  $P_{12}(\tau)$  measured in one cell, are shown in Fig. 4 *a*. At all time intervals,  $P_{12}(\tau)$  is larger than  $P_{01}(\tau)$ . The ratio  $K_{12}/K_{01}$  is equal to 1.18. In seven cells examined, the value of this ratio was  $1.12 \pm 0.08$  (mean  $\pm$  SD). Is this estimate unbiased, significantly different from one, and really discriminatory between our two models of activation?

One possible bias could have arisen from the existence, during one channel opening, of the transient closures mentioned in the Methods section, which are not taken into account in Schemes I and II. These transient interruptions, due to brief oscillations of one channel between the open and closed states, are internal to one opening and should not be considered as separate, independent openings. Is it possible that they introduce a systematic error in our estimates of  $P_{ij}(\tau)$ ? When transient closures more brief

than 2 ms (i.e., 3 to 5 times their mean duration) are discarded from the analysis, the ratio  $K_{12}/K_{01}$  becomes even larger (1.35 in Fig. 4 *b*) than before their suppression. This is also true for the average of seven experiments, where  $K_{12}/K_{01}$  equals  $1.18 \pm 0.13$  (mean  $\pm$  SD) when estimated as in Fig. 3 *b*. This shows that the transient interruption observed during one channel opening do not account for an experimental value  $K_{12}/K_{01}$  larger than one. On the contrary, since the opening of a second channel appears to be uncorrelated to the transient closures of the first one, these events will tend to mask the correlation that we study, between two successive openings.

To be confident in the precision of the estimates of the transition rates, one has to make sure that the length of analyzed data is sufficient. This was done by studying the convergence of  $K_{ij}$  toward a satisfactorily stable value, as a function of the length of data. In the example shown in Fig. 4 *c*, it was found that estimates of transition rates taking into account less than 1,000 events (openings or closings) cannot be considered as accurate enough. All our estimates of  $K_{12}$  and  $K_{01}$  were thus done after checking for their convergence to a stable value.

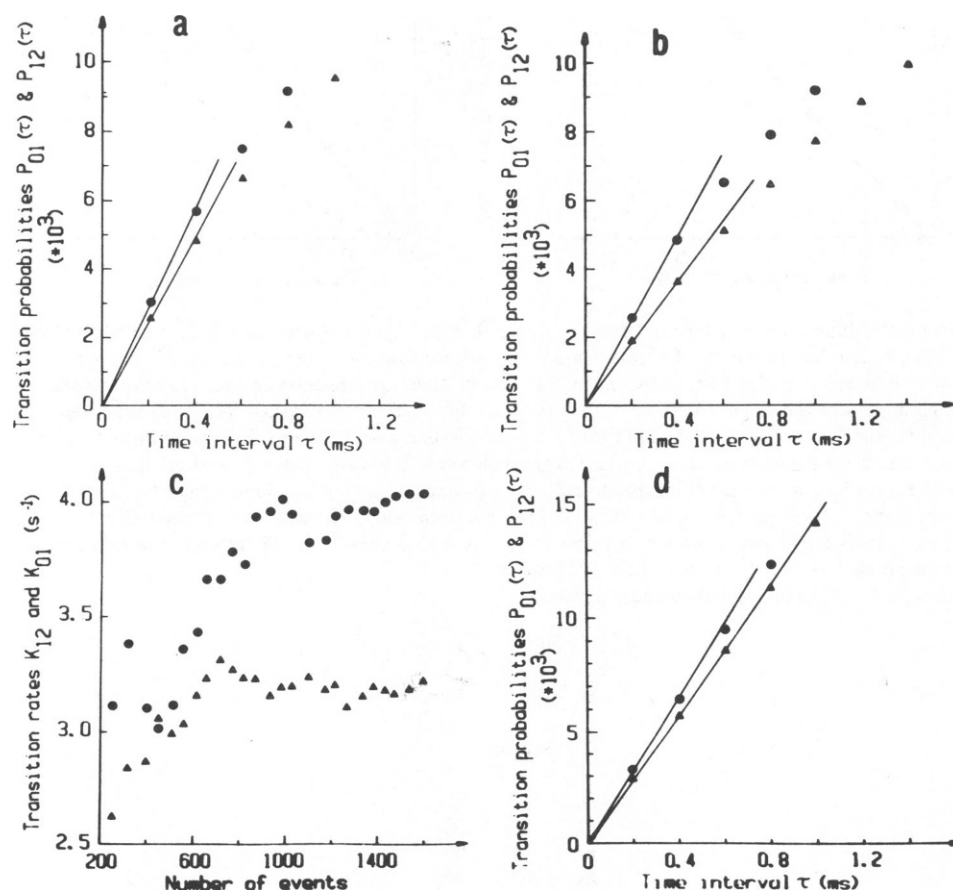


FIGURE 4 Transition probabilities and transition rates. (a) Experimental values of  $P_{01}(\tau)$  (▲) and  $P_{12}(\tau)$  (●) were obtained in one patch (as explained in the text). The transition rates, calculated as  $P_{ij}(\Delta T)/\Delta T$  with  $\Delta T = 0.2$  ms, appear as the slopes of the straight lines. (b) Experimental values of  $P_{01}(\tau)$  (▲) and  $P_{12}(\tau)$  (●) with the same data as in *a*, but after suppression of closures more brief than 2 ms. (c) Effect of the number of transitions considered on the estimates of  $K_{12}$  (●) and  $K_{01}$  (▲). (d) Values of  $P_{01}(\tau)$  (▲) and  $P_{12}(\tau)$  (●) obtained by simulation of Scheme II, assuming 15 dimers and the same parameters as in Fig. 3 *c* (where  $k_{12}/k_{01} = 10$ ). The ratio between transition rates is 1.16.



The next question was whether a ratio of 1.12 for the two transition rates reflects a significant cooperativity in the activation of two channels. One answer can be brought by simulations of the two schemes (with the constants given in the Fig. 3 legend). A simulation of Scheme I gives  $K_{12}/K_{01} = 0.93$  for 30 channels (not illustrated). A simulation of Scheme II is shown in Fig. 4 d; for 15 dimers, it gives  $K_{12}/K_{01} = 1.16$ .

Analytically (see Theory), it appears that a rather inconspicuous excess between  $K_{12}/K_{01}$  and 1 reveals a much larger discrepancy between the microscopic constants  $k_{12}$  and  $k_{01}$ . This factor between  $k_{12}/k_{01}$  and  $K_{12}/K_{01}$  depends on the number of channels in the patch. For instance, given our experimental value of the ratio of the transition rates (1.12), assuming that a patch contains 20–400 functional dimers, the ratio  $k_{12}/k_{01}$  is in the range of 5–100, in other words the rate constant of opening of a channel would be at least 5–100 times higher once its neighbor is opened.

The “diluting effect” of the number of channels on the cooperative interaction in a dimer can also be illustrated by the fact that with the figures given here and in the Theory section, a second opening would result from the activation of a dimer in between 0.5 and 10% of the cases, and from independent monomers in all the other cases.

## DISCUSSION

Here, we have demonstrated that the type of events illustrated in Fig. 2, i.e., the simultaneous opening or closing of two channels, is indeed more frequent than one would expect from mere coincidence: the ACh-activated channels in rat myotubes are not independent.

In the presentation of the results, we have used throughout this paper the concept of functional dimers. The type of interaction that we have detected could also take place between one receptor and several of its neighbors as proposed in the “lattice model” (Changeux et al., 1967). But the dimeric model has the advantage of simplicity and possesses a structural basis: in the electric organ of electric fishes, the nicotinic receptor can be found in the membrane either in a monomeric form (with five subunits arranged in an  $\alpha_2\beta\gamma\delta$  structure), or in a dimeric form, with disulfide bonds between the  $\delta$  subunits belonging to adjacent monomers (Reynold and Karlin, 1978). It would be interesting to compare the behavior of a population of monomers and of dimers. A recent report comparing monomers and dimers reconstituted in a planar bilayer (Schindler et al., 1984) have led to the conclusion that dimers with two synchronized channels should be the *in vivo* predominant gating units. This conclusion is difficult to reconcile with those of a previous report (Boheim et al., 1981) where no difference was observed between the behavior of monomers and dimers, and with the fact that substates with half conductances have not been reported in *in vivo* native membranes.

It would be of interest to know whether the functional coupling that we have demonstrated depends upon agonist concentration (in which case it could influence the shape of the dose-response curve). Unfortunately, this question is difficult to address, because of desensitization. At high agonist concentration, all the receptors can be desensitized, except for one which oscillates between the open and closed states (Sakmann et al., 1980; Siegelbaum et al., 1984). Thus, in a dimer, one receptor can be in the desensitized state and the other not. An increase in agonist concentration, by enhancing desensitization, will reduce the proportion of functional dimers and increase the proportion of functional monomers in the population of receptors. Desensitization will have a canceling effect on the coupling phenomenon, and thus prevents a simple analysis of the effect of agonist concentration on this coupling.

As far as methods go, the present study shows that independence in a population of homogeneous molecules should not be tested only by comparing experimental data to a Poisson distribution. Resorting to the two-time properties appears to be a safer procedure.

We thank S. Siegelbaum for his participation to the early part of this work, and A. Denis, A. Marty, and A. Ribera for helpful discussions and comments on the manuscript.

This work was supported by grants from the Centre National de la Recherche Scientifique, Ministère de l'Industrie et de la Recherche and Université Pierre et Marie Curie.

## APPENDIX I

Let us consider a population of  $n = n_a + n_b$  channels resulting from the addition of two populations with  $n_a$  and  $n_b$  channels, respectively. We suppose that all the channels are independent, have the same conductance, but the two populations have different kinetics. In the various parameters, the two populations are referred to by the upperscripts (a) and (b), and the total population by the upperscript (n).

Let  $P_0^{(a)}$ ,  $P_0^{(b)}$  and  $P_0^{(n)}$  be the stationary probabilities for populations a and b to have no channels open and one channel open. For the total population we have the (experimentally measured) probabilities.

$$P_0^{(n)} = P_0^{(a)} \cdot P_0^{(b)}$$

and

$$P_1^{(n)} = P_0^{(a)} \cdot P_1^{(b)} + P_1^{(a)} P_0^{(b)}$$

The macroscopic measured ratio  $K_{12}/K_{01} = \rho$  can be expressed as follows:

$$\frac{K_{12}}{K_{01}} = \frac{\frac{N_{12}^{(n)}}{P_1^{(n)}}}{\frac{N_{01}^{(n)}}{P_0^{(n)}}}$$

In this expression  $N_{ij}^{(n)}$  has the meaning given in the text.

We need to further express each  $N_{ij}^{(n)}$  as a sum of terms, denoted  $N_{kalb-mapb}/$  (with the conditions  $k+1=i$  and  $m+p=j$ ) and corresponding to the number of steps where the level  $i$  is imputable to the sum of a level  $k$  in population a and a level  $l$  in population b; an analogous decomposition

holds for level  $j$ . These decompositions lead to

$$N_{01}^{(n)} = N_{0a0b-1a0b} + N_{0a0b-0a1b}$$

and

$$N_{12}^{(n)} = N_{1a0b-1a1b} + N_{1a0b-2a0b} + N_{0a1b-1a1b} + N_{0a1b-0a2b}$$

By an extension of the development presented in the text, each term

$$\frac{N_{kalb-mapb}}{T}$$

(with  $T$  representing the total duration of the recording) can be expressed as the product of two two-time probabilities. For example

$$\frac{N_{0a0b-1a0b}}{T} = P_{01}^{(a)}(\tau) \cdot P_{00}^{(b)}(\tau)$$

and

$$\frac{N_{0a0b-1a0b}}{TP_0^{(n)}} = \frac{N_{0a0b-1a0b}}{TP_0^{(a)}P_0^{(b)}} = \left(\frac{P_{01}^{(a)}}{P_0^{(a)}}\right)\left(\frac{P_{00}^{(b)}}{P_0^{(b)}}\right) = P_{01}^{(a)}(\tau) \cdot P_{00}^{(b)}(\tau)$$

with  $\tau \rightarrow 20$ , we have

$$\lim_{\tau \rightarrow 0} \frac{1}{T\tau} \cdot \frac{N_{0a0b-1a0b}}{P_0^{(n)}} = n_a k_{01}^{(a)}.$$

By performing analogous calculations, it is possible to show that with the adopted notations, the relation  $K_{12}/K_{01} = \rho$  can be written under the form

$$\frac{1}{P_1^n} [P_1^{(a)}P_0^{(b)}n_b k_{01}^{(b)} + P_1^{(a)}P_0^{(b)}(n_a - 1)k_{01}^{(a)} + P_0^{(a)}P_1^{(b)}n_a k_{01}^{(a)} + P_0^{(a)}P_1^{(b)}(n_b - 1)k_{01}^{(b)}] = \rho [n_a k_{01}^{(a)} + n_b k_{01}^{(b)}],$$

or

$$k_{01}^{(a)} [P_1^{(a)}P_0^{(b)}(n_a - 1 - \rho n_a) + P_0^{(a)}P_1^{(b)}(n_a - \rho n_a)] + k_{01}^{(b)} [P_1^{(a)}P_0^{(b)}n_b - \rho n_b] + P_0^{(a)}P_1^{(b)}(n_b - 1 - \rho n_b) = 0$$

(equation:  $L = 0$ )

If  $\rho > 1$ , the left-hand side  $L$  of this equation is such that  $L < - (k_{01}^{(a)}P_1^{(a)}P_0^{(b)} + k_{01}^{(b)}P_0^{(a)}P_1^{(b)}) < 0$ , and thus  $\rho > 1$  is incompatible with the hypothesis of independent channels for the two populations  $a$  and  $b$ . This reasoning can be easily generalized to an arbitrary number of populations.

## APPENDIX II

Here is detailed the origin of the parabolic behavior of the two-time probability  $P_{02}^{(n)}(\tau)$  for a population of  $n$  independent channels. Let  $P_{00}^{(1)}(\tau)$  and  $P_{01}^{(1)}(\tau)$  be the two-time probabilities corresponding to one such channel. One can write

$$P_{01}^{(n)}(\tau) = n(P_{00}^{(1)}(\tau))^{n-1}P_{01}^{(1)}(\tau)$$

$$P_{02}^{(n)}(\tau) = (1/2)n(n-1)(P_{00}^{(1)}(\tau))^{n-2}(P_{01}^{(1)}(\tau))^2.$$

$(1/2)n(n-1)$  is the combinatorial factor for the choice of the two channels in the population of  $n$  that undergo the transition closed-open during the time interval  $\tau$ .

For small values  $P_{00}^{(1)}(\tau) = p_0(\infty)(1 - k_{01}\tau)$ , and  $P_{01}^{(1)}(\tau) = p_0(\infty)k_{01}\tau$  ( $p_0(\infty)$  is the stationary probability for one channel to be in the closed

state), thus for  $\tau \rightarrow 20$

$$P_{02}^{(n)}(\tau) \approx (1/2)n(n-1)(p_0(\infty))^n k_{01}^2 \tau^2 \approx A'(P_{01}^{(1)}(\tau))^2 \pm A(P_{01}^{(n)}(\tau))^2.$$

This criterion of parabolic behavior of  $P_{02}(\tau)$  for independent channels (with the condition  $\tau \rightarrow 20$ ) can be easily generalized to an arbitrary number of populations of independent channels (it is also supposed that the behavior of a channel belonging to population  $a$  does not depend on the behavior of any channel in any other population  $j$ ).

For example, with the hypotheses and notations of Appendix I, for two populations  $a$  and  $b$  one has (the superscript  $(1k)$   $k = a$  or  $b$  indexes the two-time probabilities corresponding to one channel belonging to population  $k$ )

$$\begin{aligned} P_{02}^{(n)}(\tau) &= (1/2)n_a(n_a-1)(P_{00}^{(1a)}(\tau))^{n_a-2} \\ &\quad \cdot (P_{00}^{(1b)}(\tau))^{n_b}(P_{01}^{(1a)}(\tau))^2 \\ &\quad + (1/2)n_b(n_b-1)(P_{00}^{(1a)}(\tau))^{n_a} \\ &\quad \cdot (P_{00}^{(1b)}(\tau))^{n_b-2}(P_{01}^{(1b)}(\tau))^2 \\ &\quad + n_a n_b (P_{00}^{(1a)}(\tau))^{n_a-1} \\ &\quad \cdot (P_{00}^{(1b)}(\tau))^{n_b-1}(P_{01}^{(1a)}(\tau))(P_{01}^{(1b)}(\tau)) \end{aligned}$$

and by performing the same type of calculations as for one population it is easy to see that  $P_{02}^{(n)}(\tau)$  is proportional to  $\tau^2$  for  $\tau \rightarrow 0$ .

## REFERENCES

- Boheim, G., W. Hanke, F. J. Barrantes, H. Eibl, B. Sakmann, G. Fels, and A. Maelicke. 1981. Agonist-activated ionic channels in acetylcholine receptor reconstituted into planar lipid bilayers. *Proc. Natl. Acad. Sci. USA*. 78:3586-3590.
- Changeux, J. P., J. Thiery, Y. Tung, and C. Kittel. 1967. On the cooperativity of biological membranes. *Proc. Natl. Acad. Sci. USA*. 57:335-341.
- Colquhoun, D. and A. G. Hawkes. 1977. Relaxation and fluctuations of membrane currents that flow through drug-operated channels. *Proc. R. Soc. Lond. B. Biol. Sci.* 199:231-262.
- Colquhoun, D., and B. Sakmann. 1981. Fluctuations in the microsecond time range of the current through single acetylcholine receptor ion channels. *Nature (Lond.)*. 294:464-466.
- Cox, D. R., and H. D. Miller. 1965. *The Theory of Stochastic Processes*. Chapman & Hall, New York.
- Hamill, O. P., A. Marty, E. Neher, B. Sakmann, and F. J. Sigworth. 1981. Improved patch-clamp techniques for high-resolution current recording from cells and cell-free membrane patches. *Pfluegers Arch.* 391:85-100.
- Katz, B., and S. Thesleff. 1957. A study of the desensitization produced by acetylcholine at the motor endplate. *J. Physiol. (Lond.)*. 138:60-80.
- Katz, B. and R. Miledi. 1972. The statistical nature of the acetylcholine potential and its molecular components. *J. Physiol. (Lond.)* 224:665-699.
- Land, B. R., T. R. Podleski, E. E. Salpeter, and M. M. Salpeter. 1977. Acetylcholine receptor distribution on myotubes in culture correlated to acetylcholine sensitivity. *J. Physiol. (Lond.)*. 269: 155-176.
- Neher, E., B. Sakmann, and J. H. Steinbach. 1978. The extracellular patch-clamp: a method for resolving currents through individual open channels in biological membranes. *Pfluegers Arch.* 375:219-228.
- Neher, E., and C. F. Stevens. 1977. Conductance fluctuations and ionic pores in membranes. *Annu. Rev. Biophys. Bioeng.* 6:345-381.
- Postnikov, A. G. 1973. *Selected Translations in Mathematical Statistics and Probability*. vol. 13, American Mathematical Society, editor. Providence, Rhode Island. 41-122.

- Reynold, J. A., and A. Karlin. 1978. Molecular weight in detergent solution of acetylcholine receptor from *Torpedo californica*. *Biochemistry*. 17:2035–2038.
- Sakmann, B., J. Patlak, and E. Neher. 1980. Single acetylcholine-activated channels show burst-kinetics in presence of desensitizing concentrations of agonist. *Nature (Lond.)*. 286:71–73.
- Schindler, H., F. Spillecke, and E. Neumann. 1984. Different channel properties of *Torpedo* acetylcholine receptor monomers and dimers reconstituted in planar membranes. *Proc. Natl. Acad. Sci. USA*. 81:6222–6226.
- Siegelbaum, S., A. Trautmann, and J. Koenig. 1984. Single acetylcholine-activated channel currents in developing muscle cells. *Dev. Biol.* 104:366–379.
- Takeda, K., and A. Trautmann. 1984. A patch-clamp study of the partial agonist actions of tubocurarine on rat myotubes. *J. Physiol.(Lond.)*. 349:353–374.
- Tank, D. W., C. Miller, and W. W. Webb. 1982. Isolated-patch recording from liposomes containing functionally reconstituted chloride channels from *Torpedo* electroplax. *Proc. Natl. Acad. Sci. USA*. 78:7749–7753.